International Journal of Microwave and Wireless Technologies

cambridge.org/mrf

Compact UWB BPF with a notched band using a single perturbed HMSIW cavity

Lili Qu, Yonghong Zhang, Qun Li and Yong Fan

Department of Microwave Engineering, University of Electronic Science and Technology of China, Chengdu 611731, China

Research Paper

Cite this article: Qu L, Zhang Y, Li Q, Fan Y (2020). Compact UWB BPF with a notched band using a single perturbed HMSIW cavity. *International Journal of Microwave and Wireless Technologies* **12**, 809–814. https://doi.org/10.1017/S1759078720000252

Received: 3 May 2019
Revised: 4 March 2020
Accepted: 5 March 2020
First published online: 31 March 2020

Key words:
Bandpass filter; half-mode substrate-integrated waveguide (HMSIW); notched band; ultra-wideband (UWB)

Author for correspondence:
Yonghong Zhang,
E-mail: zhangyhh@uestc.edu.cn

Abstract

This paper presents a notched band ultra-wideband bandpass filter using a single perturbed quint-mode half-mode substrate-integrated waveguide cavity. The cavity is perturbed by loading four stubs at two corners of the magnetic walls of the single cavity. The variable parameters of stubs are selected to move down the first five resonant modes to the predetermined passband during the design process. Meanwhile, microstrip lines with a transition structure located on two loaded stubs are employed to feed the resonator. Moreover, the filter also firstly designs a notched band by introducing a complementary split-ring resonator inside the cavity to mitigate potential interference signals at 8 GHz (satellite communication). Finally, a prototype filter was implemented and measured to verify.

Introduction

With the development of wireless communications, microwave filters are key components to select frequency signals [1, 2]. Ultra-wideband (UWB) bandpass filters (BPFs) have been a hot topic in the UWB system front end since they affect the performance of the entire system [3, 4]. Multi-mode resonator (MMR) technology and highpass–lowpass combination technology are widely used to implement UWB filters [5–13]. However, compared with highpass–lowpass combination technology, there have been few attempts to design substrate-integrated waveguide (SIW) UWB BPFs in MMR technology, and these filters are confronted with complex design procedures, large circuit sizes, multi-layer structures, and undesirable interference problems [11–13]. In [11], a UWB BPF is designed using hybrid half-mode SIW (HMSIW) – microstrip hybrid structure. However, the structure has a deteriorated quality factor, and it suffers undesired interference caused by coexisting wireless services, which can be mitigated by using a notch structure. A UWB filter using a SIW ridged MMR integrated on the multi-layer structure is designed in [12]. However, the undesired interference within the passband has not been mitigated. In [13], a notch-band wideband BPF integrated on a multi-layer SIW circuit was designed using a quad-mode one-third isosceles triangular resonator, but it covered a limited 3 dB fractional bandwidth (FBW), only accounts for 33.33%, which cannot adequately supply a UWB passband. In addition, multi-layer SIW structure implementations are challenged by alignment and fabrication complexity problems [12, 13]. Until now, the design of UWB BPF based on a planar SIW MMR is a big challenge.

On the other hand, defected ground structure (DGS) embedded inside the SIW structure are commonly utilized to create UWB passbands [5–11], rather than notched bands within the UWB passbands. In [6, 10, 13], although the notched bands are reported using DGS embedded inside HMSIW or SIW circuit, this approach is applied to design bandstop filters, rather than notched bands within UWB passbands. The notched bands within SIW wide passbands are designed by introducing extra circuits outside the SIW structure [14, 15], which undoubtedly requires an additional circuit for notch structure so that large-scale circuit layout is inevitable. To the best of the authors' knowledge, no paper has been reported about the realization of notched bands within a UWB passband using DGS embedded inside the SIW circuit.

This paper firstly proposes a perturbed HMSIW cavity resonator and its single-cavity application to design a UWB BPF with a notched band using a complementary split-ring resonator (CSRR). Five resonant modes are perturbed using four loaded stubs, and they are allocated to the specified frequencies in the UWB passband. In addition, a CSRR embedded inside HMSIW is employed to construct a notched band for the first time. The proposed filter is very suitable for UWB system applications.

Design procedures

HMSIW resonator

Figure 1(a) shows the geometric layout of a square HMSIW resonator. It consists of three magnetic boundaries and an electric boundary [16]. The even/odd mode theory is adopted to

© Cambridge University Press and the European Microwave Association 2020

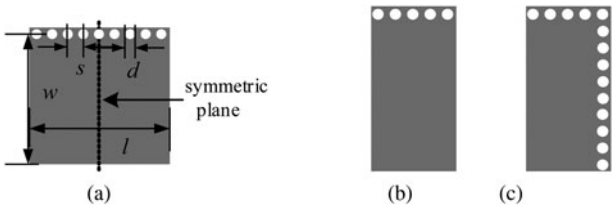


Fig. 1. (a) Layout of the HMSIW resonator, (b) even-mode and (c) odd-mode model of the resonator, $d = 0.6$, $s = 0.9$, $w = 9.45$, and $l = 9.45$ (all in mm).

analyze its working mechanism owing to its symmetry structure. The even-mode equivalent model in Fig. 1(b) not only transmits SIW cavity resonant mode – TE102 mode, but also can be regarded as a short-circuited quarter wavelength microstrip-line resonator transmitting quasi-TEM mode. The resonance frequencies of the fundamental and higher quasi-TEM modes can be calculated by using the transmission line theory [17].

$$f_{e(1,0,0)} = \frac{c_0}{4w\sqrt{\varepsilon_r}}, \tag{1}$$

$$f_{e(3,0,0)} = \frac{3c_0}{4w\sqrt{\varepsilon_r}}, \tag{2}$$

while that of the TE102 mode can be calculated by

$$f_{e102} = \frac{c_0\sqrt{17}}{4\sqrt{\varepsilon_r}w}. \tag{3}$$

The odd-mode equivalent structure excitation in Fig. 1(c) is equivalent to a quarter-mode SIW resonator providing TE101 and TE103 modes, whose resonance frequencies are extracted by

$$f_{o101} = \frac{c_0\sqrt{5}}{4\sqrt{\varepsilon_r}w}, \tag{4}$$

$$f_{o103} = \frac{c_0\sqrt{13}}{4\sqrt{\varepsilon_r}w}, \tag{5}$$

where c_0 is the speed of light in free space and ε_r is the relative permittivity of the dielectric substrate. The dimensions of the resonator can be calculated by (1–5) with $w = l = 9.45$ mm. Using the commercial electromagnetic simulation software HFSS, the electric field distribution of the first five degenerate modes are obtained, as shown in Fig. 2. They can be differentiated as even or odd modes based on their electric field distributions at the symmetrical region. Due to the strong electric field distributions

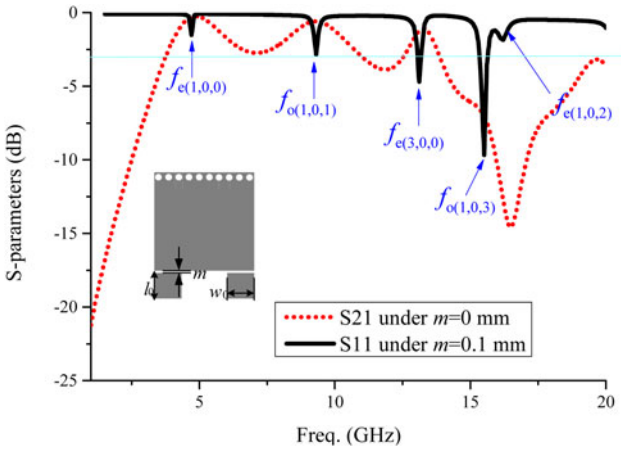


Fig. 3. Transmission response of the HMSIW bandpass filter, $w_0 = 1.13$ and $l_0 = 1$ (all in mm).

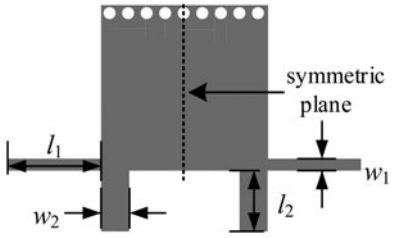


Fig. 4. Layout of the perturbed HMSIW resonator.



Fig. 5. Models (a) even-mode and (b) odd-mode.

at the symmetrical region, the first and third resonant modes are characterized as even modes transmitting quasi-TEM, as shown in Figs 2(a) and 2(c), while that of another even mode transmitting TE102 mode is shown in Fig. 2(e). Likewise, Figs 2(b) and 2(d) depict the electric field distributions of the first two odd modes, TE101 and TE103, respectively.

The transmission response of the HMSIW BPF without any perturbation is depicted in Fig. 3. The microstrip feed lines with a width of w_0 and a length of l_0 are arranged at two corners

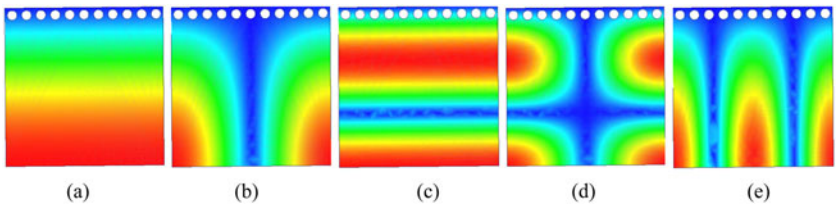


Fig. 2. Electric field magnitude distributions of the first five resonant modes, (a) even mode 1, (f_{e1}), (b) odd mode 1 (f_{o1}), (c) even mode 2, (f_{e2}), (d) odd mode 2, (f_{o2}), and (e) even mode 3, (f_{e3}).

https://doi.org/10.1017/S1759078720000252 Published online by Cambridge University Press

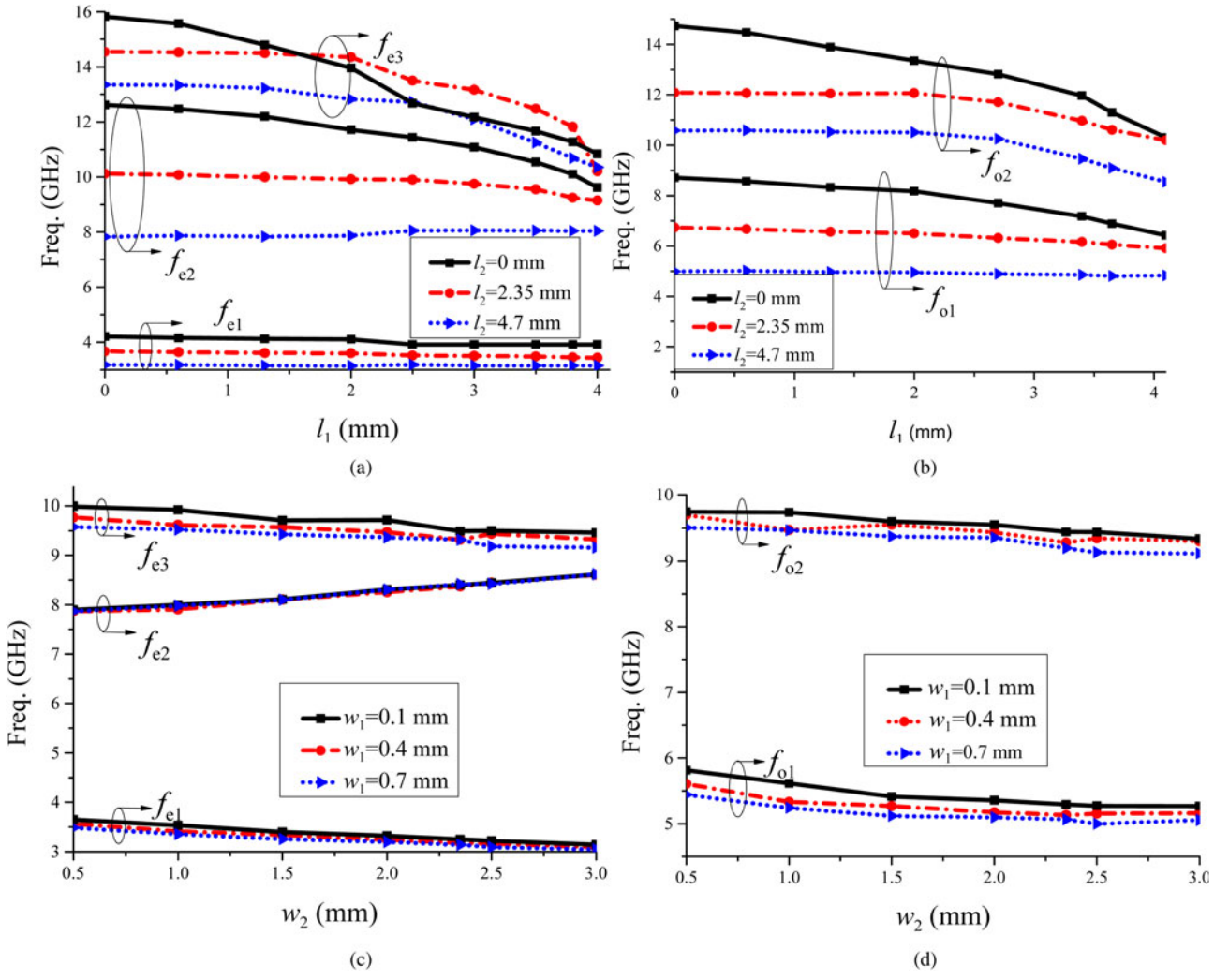


Fig. 6. Resonance frequencies characteristics of (a) even modes varying with l_1, l_2, (b) odd modes varying with l_1, l_2, (c) even modes varying with w_1, w_2, and (d) odd modes varying with w_1, w_2.

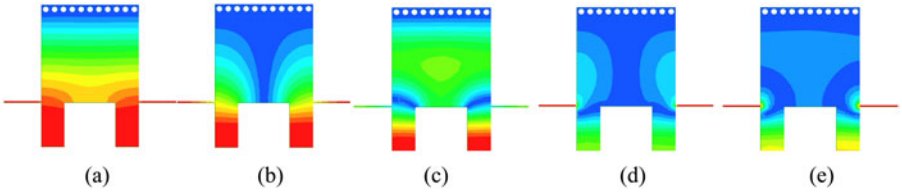


Fig. 7. Electric field magnitude distributions of the first five resonant modes (a) even mode 1, (f_{e1}), (b) odd mode 1 (f_{o1}), (c) even mode 2, (f_{e2}), (d) odd mode 2, (f_{o2}) and (e) even mode 3, (f_{e3}).

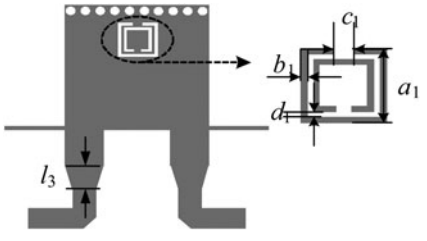


Fig. 8. Layout of the proposed notched band UWB BPF.

formed by the magnetic walls. As can be seen, a transmission zero (TZ) is generated at the upper stopband due to the excitation of higher order modes in the cavities. However, the resonant frequencies of the first five modes are too far to form a bandpass frequency response. To improve the performance of the filter, the perturbation technique will be presented and analyzed in the following sections.

Perturbed HMSIW resonator

The configuration of the perturbed HMSIW resonator is presented in Fig. 4, which is constructed by loading four stubs on the two corners formed by the magnetic walls. The working principle of the conventional HMSIW resonator can be applied to analyze the proposed resonator.

https://doi.org/10.1017/S1759078720000252 Published online by Cambridge University Press

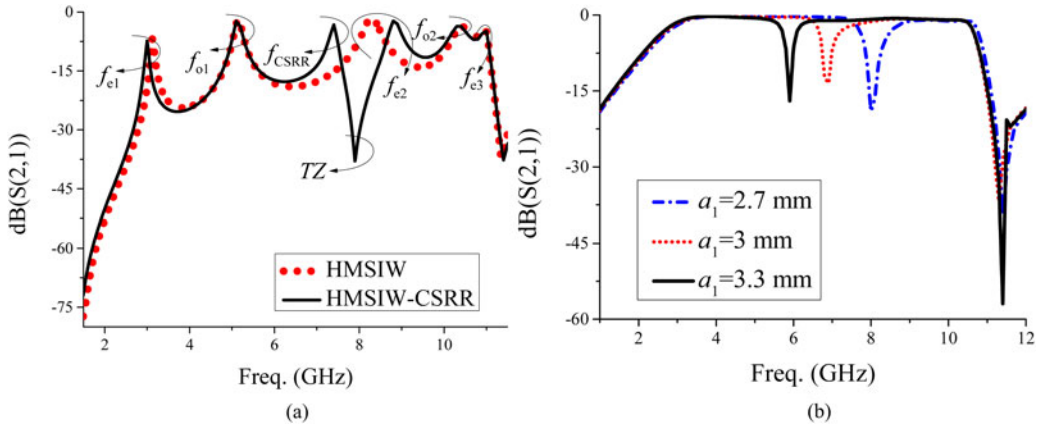


Fig. 9. (a) Simulated *S*21 of HMSIW-CSRR under weak coupling, and (b) simulated *S*21 of HMSIW-CSRR varying with a_1.

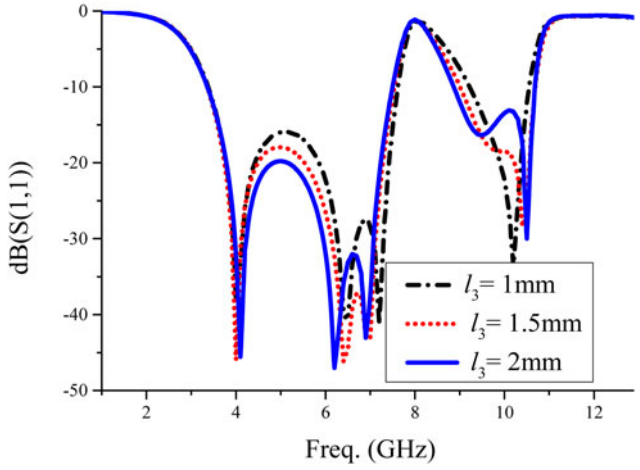


Fig. 10. Simulated *S*11 varying with l_3.

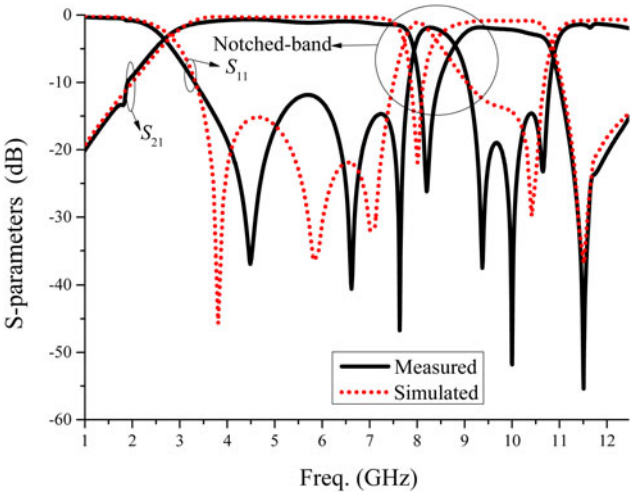


Fig. 12. Simulated and measured *S*-parameters of the fabricated filter.

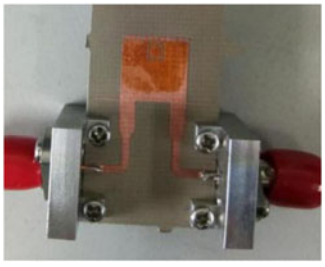


Fig. 11. Photograph of the fabricated filter.

Even/odd mode theory is also utilized as shown in Figs 5(a) and 5(b). According to the models shown in Figs 1(b) and 1(c), the working area of the actual circuit is increased with the loaded stubs, thus the frequencies of TEm0p modes are reduced. For the quasi-TEM mode excitation in Fig. 5(a), the loaded stubs make the circuit behave as a short-circuited stepped-impedance resonator, which can effectively reduce the frequencies of high harmonics thereby further reducing the circuit size. To illustrate clearly, the frequency response of the first five resonant modes, three even modes and two odd modes, versus l_1, l_2, w_1, and w_2 is investigated in Fig. 6. In Figs 6(a) and 6(b), w_1 and w_2 are set as 0.15 and 2.34 mm, respectively. In Figs 6(c) and 6(d), $l_1$and l_2 are set as 3.8 and 4.5 mm, respectively. As can be seen, the resonant frequencies decrease greatly with the increase of l_1 and l_2, while they decrease slowly with the increase of w_1 and w_2. Based on the curves and equations, the variable parameters, l_1, l_2, w_1, and w_2, are selected to provide five resonant modes within the predetermined passband during the tuning process.

Figure 7 presents the electric field magnitude distributions at the five resonant modes. As can be seen, the electric field magnitude distributions of mode (1–3) are strong at the loaded stubs, while that of mode (4–5) is a little weak. Therefore, strong external coupling can be implemented by locating the microstrip feed lines on two broad-edge loaded stubs.

Notched band design

To implement a notched band within the UWB passband, a CSRR embedded inside the SIW circuit is firstly proposed, whose geometrical structure is shown in Fig. 8. It consists of a UWB BPF geometrical structure and a CSRR etched on the HMSIW top metal plane. A transmission pole (TP) would be produced when the CSRR is excited by the HMSIW resonator.

https://doi.org/10.1017/S1759078720000252 Published online by Cambridge University Press

Table 1. Comparisons with previous UWB BPFs

Ref.	Size ($\lambda g \times \lambda g$)	3 dB FBW (%)	IL (dB)	Notch Freq. (GHz)	Notch allocation
[8]	2.46 × 0.29	103.5	<1.63	No	No
[9]	1.34 × 1.64	114	<1.2	5.51	Outside
[10]	0.87 × 0.66	111.3	<1.77	5.8	Outside
[11]	0.93 × 0.11	92.3	<1.74	No	No
[12]	0.54 × 0.6	110	<1	No	No
[13]	1.56 × 2.08	33.33	NA	15.5	Outside
Proposed	0.54 × 0.66	117.2	<2.4	8	Inside

Meanwhile, the coupling between the CSRR and the resonator is mixed electromagnetic coupling, and hence producing a TZ. By allocating the TZ within the passband, a notched band would be implemented. To demonstrate clearly, Fig. 9(a) depicts the simulated *S*-parameters of HMSIW and HMSIW-CSRR under weak coupling, respectively. An extra TP and a TZ could be clearly observed, which are consistent with the predicted results. In this way, allocating the TZ within the passband can generate a notched band. From Fig. 9(b), we can find that the position of notched bands can be flexibly controlled with varied a_1. Due to the working mechanism, the bandwidth of the notch can be controlled by controlling its external coupling, which can be controlled by the geometrical structure of CSRR. Therefore, this method is validated for designing a notched band.

Meanwhile, the tapered transition between the stub and the inputs transition structure is designed for a better impedance match. Figure 10 shows the return loss of the proposed filter against varied l_3. Slight offset of resonance frequency can be observed due to the influence of loaded tapered lines.

Verify

To verify, a UWB BPF with a notched band is designed, fabricated, and measured. The photograph of the fabricated filter is shown in Fig. 11. The filter is fabricated on the Taconic RF-35 substrate with a thickness of 0.508 mm, a relative dielectric constant of 3.5, and a loss tangent of 0.0018. The measured and simulated *S*-parameters of the proposed filter are plotted in Fig. 12, showing good consistency between them. Small discrepancies are observed owing to the tolerance of fabrication. The optimized overall geometrical dimensions are $w = 9.9$, $l_1 = 3.85$, $w_1 = 0.15$, $l_2 = 4$, $w_2 = 2.34$, $l_3 = 1$, $a_1 = 2.7$, $c_1 = 0.2$, $d_1 = 0.2$, $b_1 = 0.2$, $l_0 = 1$, $w_0 = 1.13$, $d = 0.6$, and $s = 0.9$ (all in mm). The measured frequency range is 2.75–10.53 GHz, and its 3 dB FBW is about 117.2%. The notch band centering at 8 GHz has a 3 dB FBW of 13.1%. A comparison with other reported SIW UWB filters is shown in Table 1, which demonstrates the proposed filter has good performance and smaller size.

Conclusion

A compact UWB BPF with a notched band using a perturbed quint-mode HMSIW resonator and a CSRR is presented in this paper. The resonator is developed by embedding four stubs on the end of HMSIW magnetic walls and a CSRR is introduced in HMSIW metal surface to produce a controllable notched band. The validity of the design method has been confirmed by the good simulation results and the measured results.

Acknowledgement. This work was supported in part by the Ministry of Science and Technology of the People's Republic of China under grant 2013YQ200503.

References

1. **Li Q, Zhang YH, Li DT and Li Joshua LW** (2015) Miniaturized tri-band bandpass filters based on multi-mode resonators with pseudo-interdigital structure. *Electromagnetics* **35**, 488–497.
2. **Li Q, Zhang YH, Feng X and Fan Y** (2016) Tri-band filter with multiple transmission zeros and controllable bandwidths. *International Journal of Microwave and Wireless Technologies* **8**, 9–13.
3. **Wei F, Wu QY, Shi XW and Li C** (2011) Compact UWB bandpass filter with dual notched bands based on SCRLH resonator. *IEEE Microwave and Wireless Components Letters* **21**, 28–30.
4. **Wei F, Xu L, Shi XW and Liu B** (2010) Compact UWB bandpass filter with two notch-bands based on folded SIR. *Electronics Letters* **46**, 1679–1680.
5. **Rui SC, Wong SW, Zhu L and Chu QX** (2015) Wideband bandpass filter using U-slotted substrate integrated waveguide (SIW) cavities. *IEEE Microwave and Wireless Components Letters* **25**, 1–3.
6. **Esmaeili M and Bornemann J** (2017) A SIW-DGS wideband bandpass filter with a sharp roll-off at upper stopband. *Microwave and Optical Technology Letters* **59**, 789–792.
7. **Che W, Li C, Deng K and Yang L** (2008) A novel bandpass filter based on complementary split rings resonators and substrate integrated waveguide. *Microwave and Optical Technology Letters* **50**, 699–701.
8. **Huang LW and Zhang SF** (2018) Ultra-wideband ridged half-mode folded substrate-integrated waveguide filters. *IEEE Microwave and Wireless Components Letters* **28**, 579–581.
9. **Chu H and Shi XQ** (2011) Compact ultra-wideband bandpass filter based on SIW and DGS technology with a notch band. *Journal of Electromagnetic Waves and Applications* **25**, 589–596.
10. **Ding C, Wei F, Li J and Shi XW** (2015) Compact UWB BPF with notch band based on SW-HMSIW. *Electronics Letters* **51**, 1338–1133.
11. **Zhou CX, Guo PP, Zhou K and Wu W** (2017) Design of a compact UWB filter with high selectivity and superwide stopband. *IEEE Microwave and Wireless Components Letters* **27**, 636–638.
12. **Honari MM, Mirzavand R, Saghlatoon H and Mousavi P** (2017) Two-layered substrate integrated waveguide filter for UWB applications. *IEEE Microwave and Wireless Components Letters* **27**, 633–635.
13. **Zhang XJ, Zhang H and Chen YM** (2018) Design of wideband LTCC BPF with notch band exploiting one-third isosceles triangular resonator. *Microwave and Optical Technology Letters* **60**, 1403–1406.
14. **Hinojosa J, Rossi M, Saura-Rodenas A, Alvarez-Melcon A and Martinez-Viviente FL** (2018) Compact bandstop half-mode substrate integrated waveguide filter based on a broadside-coupled open split-ring resonator. *IEEE Transactions on Microwave Theory and Techniques* **66**, 3001–3010.

https://doi.org/10.1017/S1759078720000252 Published online by Cambridge University Press

15. **Esmaeili M and Bornemann J** (2017) Novel tunable bandstop resonators in SIW technology and their application to a dual-bandstop filter with one tunable stopband. *IEEE Microwave and Wireless Components Letters* **27**, 40–42.
16. **Chen F, Song K, Hu B and Fan Y** (2014) Compact dual-band bandpass filter using HMSIW resonator and slot perturbation. *IEEE Microwave and Wireless Components Letters* **24**, 686–688.
17. **Wang S, Zhang D, Zhang Y, Qing L and Zhou D** (2017) Novel dual-mode bandpass filters based on SIW resonators under different boundaries. *IEEE Microwave and Wireless Components Letters* **27**, 28–30.



Lili Qu received the B.S. degree from the Henan Normal University, Xinxiang, China, in 2014. She is currently pursuing the Ph.D. degree in Electromagnetics and Microwave Technology with the EHF Key Laboratory of Fundamental Science, School of Electronic Engineering, University of Electronic Science and Technology of China (UESTC), Chengdu, China. Her research interests include antennas, electromagnetic theory, and microwave circuits and systems.



Yonghong Zhang received the B. E., M.S., and Ph.D. degrees from the University of Electronic Science and Technology of China (UESTC), Chengdu, China, in 1992, 1995, and 2001, respectively. From 1995 to 2002, he was a Lecturer with UESTC. From 2002 to 2004, he was a Post-Doctoral Fellow with the Department of Electronic Engineering, Tsinghua University, Beijing, China. Since 2004, he has rejoined UESTC. He is currently a Full Professor with the School of Electronic Engineering. He has authored or coauthored more than 100 internationally refereed journal and conference papers. He is a Senior Member of the Chinese Institute of Electronics. His research interests are in the area of microwave and millimeter-wave technology and applications.



Qun Li received the B.S. degree in electronic information science and technology from the Southwest Petroleum University, Chengdu, China, in 2012, and the Ph.D. degree in electromagnetic field and microwave technology from the University of Electronic Science and Technology of China (UESTC), Chengdu, China, in 2018. In 2017, he joined the Department of Electrical and Computer Engineering, Wayne State University, Detroit, MI, USA, as a research scholar. From 2017 to 2018, he was a research scholar with the Department of Electrical and Computer Engineering, Rutgers University, New Brunswick, NJ, USA. His current research interests include antennas, electromagnetic theory, and microwave circuits and systems.



Yong Fan received the B.E. degree from the Nanjing University of Science and Technology, Nanjing, China, in 1985, and the M.S. degree from the University of Electronic Science and Technology of China (UESTC), Chengdu, China, in 1992. Since 1989, he has started to do research and teaching at UESTC. He is currently a Full Professor with the School of Electronic Engineering, UESTC. He has authored or coauthored more than 200 internationally refereed journal and conference papers. He is a Senior Member of the Chinese Institute of Electronics. His main research fields include electromagnetic theory, microwave and millimeter-wave communication, millimeter-wave and Terahertz Circuits, etc. Besides, he was interested in other subjects including Broadband Wireless Access, automobile anti-collision, intelligent transportation, etc.

https://doi.org/10.1017/S1759078720000252 Published online by Cambridge University Press